Super-Resolution Image Reconstruction:

A Technical Overview

©DIGITAL VISION, LTD.

In most electronic imaging applications, images with high resolution (HR) are desired and often required. HR means that pixel density within an image is high, and therefore an HR image can offer more details that may be critical in various applications. For example, HR medical images are very helpful for a doctor to make a correct diagnosis. It may be easy to distinguish an object from similar ones using HR satellite images, and the performance of pattern recognition in computer vision can be improved if an HR image is provided. Since the 1970s, charge-coupled device (CCD) and CMOS image sensors have been widely used to capture digital images. Although these sensors are suitable for most imaging applications, the current resolution level and consumer price will not satisfy the future demand. For example, people want an inexpensive HR digital camera/camcorder or see the price gradually reduce, and scientists often need a very HR level close to that of an analog 35 mm film that has no visible artifacts when an image is magnified. Thus, finding a way to increase the current resolution level is needed.

The most direct solution to increase spatial resolution is to reduce the pixel size (i.e., increase the number of pixels per unit area) by sensor manufacturing techniques. As the pixel size decreases, however, the amount of light available also decreases. It generates shot noise that de-grades the image quality severely. To reduce the pixel size without suffering the effects of shot noise, therefore, there exists the limitation of the pixel size reduction, and the optimally limited pixel size is estimated at about 40 μm^2 for a 0.35 μm CMOS process. The current image sensor technology has almost reached this level.

Another approach for enhancing the spatial resolution is to increase the chip size, which leads to an increase in capacitance [1]. Since large capacitance makes it difficult to speed up a charge transfer rate, this approach is not considered effective. The high cost for high precision optics and image sensors is also an important concern in many commercial applications regarding HR imaging. Therefore, a new approach toward increasing spatial resolution is required to overcome these limitations of the sensors and optics manufacturing technology.

One promising approach is to use signal processing techniques to obtain an HR image (or sequence) from observed multiple low-resolution (LR) images. Recently, such a resolution enhancement approach has been one of the most active research areas, and it is called super resolution (SR) (or HR) image reconstruction or simply resolution enhancement in the literature [1]-[61]. In this article, we use the term "SR image reconstruction" to refer to a signal processing approach toward resolution enhancement because the term "super" in "super

*Sung Cheol Park, Min Kyu Park,
and Moon Gi Kang*

resolution" represents very well the characteristics of the technique overcoming the inherent resolution limitation of LR imaging systems. The major advantage of the signal processing approach is that it may cost less and the existing LR imaging systems can be still utilized. The SR image reconstruction is proved to be useful in many practical cases where multiple frames of the same scene can be obtained, including medical imaging, satellite imaging, and video applications. One application is to reconstruct a higher quality digital image from LR images obtained with an inexpensive LR camera/camcorder for printing or frame freeze purposes. Typically, with a camcorder, it is also possible to display enlarged frames successively. Synthetic zooming of region of interest (ROI) is another important application in surveillance, forensic, scientific, medical, and satellite imaging. For surveillance or forensic purposes, a digital video recorder (DVR) is currently replacing the CCTV system, and it is often needed to magnify objects in the scene such as the face of a criminal or the licence plate of a car. The SR technique is also useful in medical imaging such as computed tomography (CT) and magnetic resonance imaging (MRI) since the acquisition of multiple images is possible while the resolution quality is limited. In satellite imaging applications such as remote sensing and LANDSAT, several images of the same area are usually provided, and the SR technique to improve the resolution of target can be considered. Another application is conversion from an NTSC video signal to an HDTV signal since there is a clear and present need to display a SDTV signal on the HDTV without visual artifacts.

How can we obtain an HR image from multiple LR images? The basic premise for increasing the spatial resolution in SR techniques is the availability of multiple LR images captured from the same scene (see [4, chap. 4] for details). In SR, typically, the LR images represent differ-

ent "looks" at the same scene. That is, LR images are subsampled (aliased) as well as shifted with subpixel precision. If the LR images are shifted by integer units, then each image contains the same information, and thus there is no new information that can be used to reconstruct an HR image. If the LR images have different subpixel shifts from each other and if aliasing is present, however, then each image cannot be obtained from the others. In this case, the new information contained in each LR image can be exploited to obtain an HR image. To obtain different looks at the same scene, some relative scene motions must exist from frame to frame via multiple scenes or video sequences. Multiple scenes can be obtained from one camera with several captures or from multiple cameras located in different positions. These scene motions can occur due to the controlled motions in imaging systems, e.g., images acquired from orbiting satellites. The same is true of uncontrolled motions, e.g., movement of local objects or vibrating imaging systems. If these scene motions are known or can be estimated within subpixel accuracy and if we combine these LR images, SR image reconstuction is possible as illustrated in Figure 1.

In the process of recording a digital image, there is a natural loss of spatial resolution caused by the optical distortions (out of focus, diffraction limit, etc.), motion blur due to limited shutter speed, noise that occurs within the sensor or during transmission, and insufficient sensor density as shown in Figure 2. Thus, the recorded image usually suffers from blur, noise, and aliasing effects. Although the main concern of an SR algorithm is to reconstruct HR images from undersampled LR images, it covers image restoration techniques that produce high quality images from noisy, blurred images. Therefore, the goal of SR techniques is to restore an HR image from several degraded and aliased LR images.

A related problem to SR techniques is image restoration, which is a well-established area in image processing applications [62]-[63]. The goal of image restoration is to recover a degraded (e.g., blurred, noisy) image, but it does not change the size of image. In fact, restoration and SR reconstruction are closely related theoretically, and SR reconstruction can be considered as a second-generation problem of image restoration.

Another problem related to SR reconstruction is image interpolation that has been used to increase the size of a single image. Although this field has been extensively studied [64]-[66], the quality of an image magnified from an aliased LR image is inherently limited even though the ideal sinc basis function is employed. That is, single image interpolation
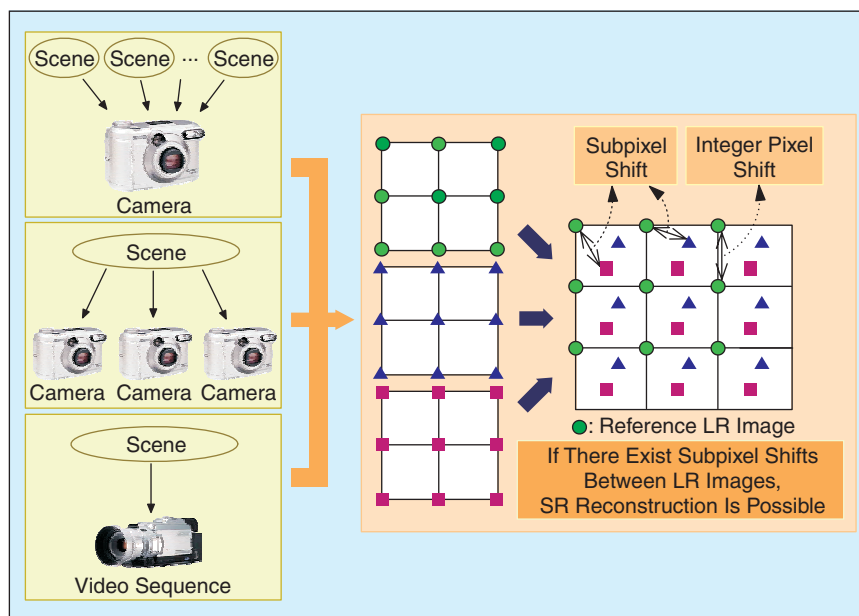
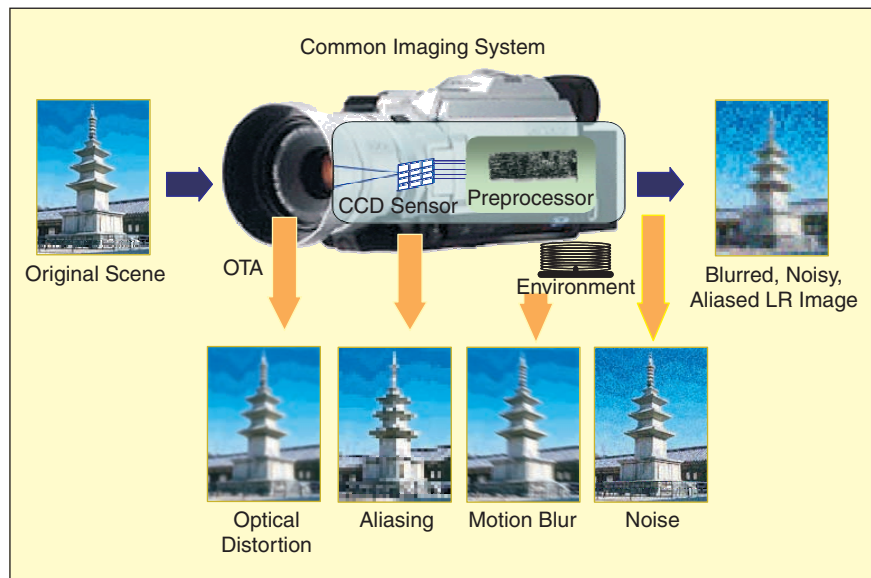▲ 1. Basic premise for super resolution.

cannot recover the high-frequency components lost or degraded during the LR sampling process. For this reason, image interpolation methods are not considered as SR techniques. To achieve further improvements in this field, the next step requires the utilization of multiple data sets in which additional data constraints from several observations of the same scene can be used. The fusion of information from various observations of the same scene allows us SR reconstruction of the scene.

The goal of this article is to introduce the concept of SR algorithms to readers who are unfamiliar with this area and to provide a review for experts. To this purpose, we present the technical review of various existing SR methodologies which are often employed. Before presenting the review of existing SR algorithms, we first model the LR image acquisition process.

▲ 2. Common image acquisition system.

Observation Model

The first step to comprehensively analyze the SR image reconstruction problem is to formulate an observation model that relates the original HR image to the observed LR images. Several observation models have been proposed in the literature, and they can be broadly divided into the models for still images and for video sequence. To present a basic concept of SR reconstruction techniques, we employ the observation model for still images in this article, since it is rather straightforward to extend the still image model to the video sequence model.

Consider the desired HR image of size $L_1 N_1 \times L_2 N_2$ written in lexicographical notation as the vector $\mathbf{x} = [x_1, x_2, ..., x_N]^T$, where $N = L_1 N_1 \times L_2 N_2$. Namely, $\mathbf{x}$ is the ideal undegraded image that is sampled at or above the Nyquist rate from a continuous scene which is assumed to be bandlimited. Now, let the parameters L_1 and L_2 represent the down-sampling factors in the observation model for the horizontal and vertical directions, re-

spectively. Thus, each observed LR image is of size $N_1 \times N_2$. Let the kth LR image be denoted in lexicographic notation as $\mathbf{y}_k = [y_{k,1}, y_{k,2}, ..., y_{k,M}]^T$, for $k = 1, 2, ..., p$ and $M = N_1 \times N_2$. Now, it is assumed that $\mathbf{x}$ remains constant during the acquisition of the multiple LR images, except for any motion and degradation allowed by the model. Therefore, the observed LR images result from warping, blurring, and subsampling operators performed on the HR image $\mathbf{x}$. Assuming that each LR image is corrupted by additive noise, we can then represent the observation model as [30], [48]

$$\mathbf{y}_k = \mathbf{DB}_k \mathbf{M}_k \mathbf{x} + \mathbf{n}_k \quad \text{for} \quad 1 \leq k \leq p \quad (1)$$

where $\mathbf{M}_k$ is a warp matrix of size $L_1 N_1 L_2 N_2 \times L_1 N_1 L_2 N_2$, $\mathbf{B}_k$ represents a $L_1 N_1 L_2 N_2 \times L_1 N_1 L_2 N_2$ blur matrix, $\mathbf{D}$ is a $(N_1 N_2)^2 \times L_1 N_1 L_2 N_2$ subsampling matrix, and $\mathbf{n}_k$ represents a lexicographically ordered noise vector. A block diagram for the observation model is illustrated in Figure 3.

Let us consider the system matrix involved in (1). The motion that occurs during the image acquisition is represented by warp matrix $\mathbf{M}_k$. It may contain global or local translation, rotation, and so on. Since this information is
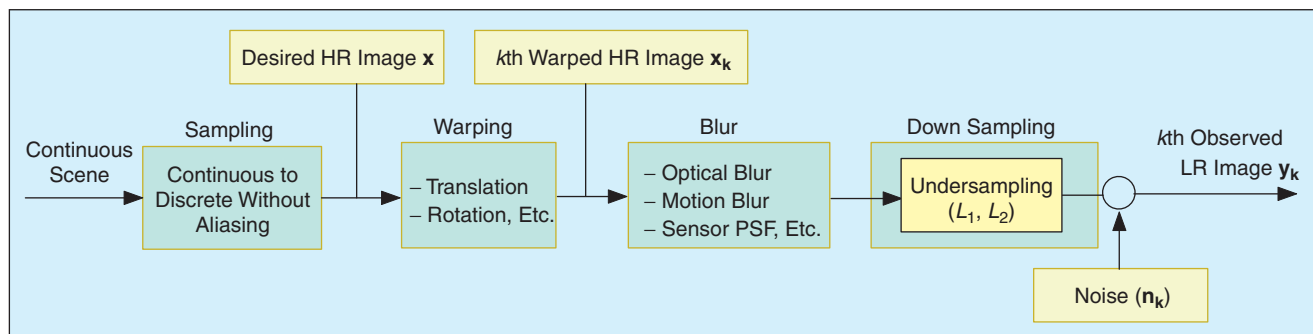

▲ 3. Observation model relating LR images to HR images.

The SR image reconstruction is proved to be useful in many practical cases where multiple frames of the same scene can be obtained, including medical imaging, satellite imaging, and video applications.

generally unknown, we need to estimate the scene motion for each frame with reference to one particular frame. The warping process performed on HR image **x** is actually defined in terms of LR pixel spacing when we estimate it. Thus, this step requires interpolation when the fractional unit of motion is not equal to the HR sensor grid. An example for global translation is shown in Figure 4. Here, a circle (○) represents the original (reference) HR image **x**, and a triangle (△) and a diamond (◇) are globally shifted versions of **x**. If the down-sampling factor is two, a diamond (◇) has $(0.5, 0.5)$ subpixel shift for the horizontal and vertical directions and a triangle (△) has a shift which is less than $(0.5, 0.5)$. As shown in Figure 4, a diamond (◇) does not need interpolation, but a triangle (△) should be interpolated from **x** since it is not located on the HR grid. Although one could use ideal interpolation theoretically, in practice, simple methods such as
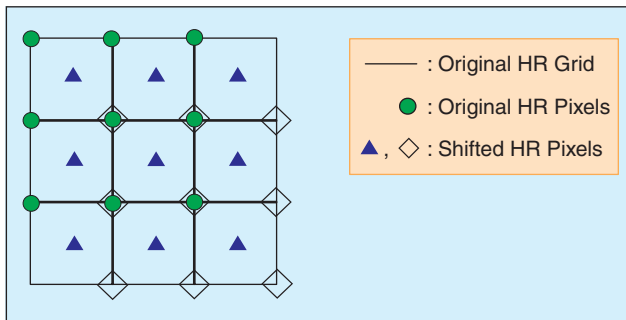
▲ 4. The necessity of interpolation in HR sensor grid.
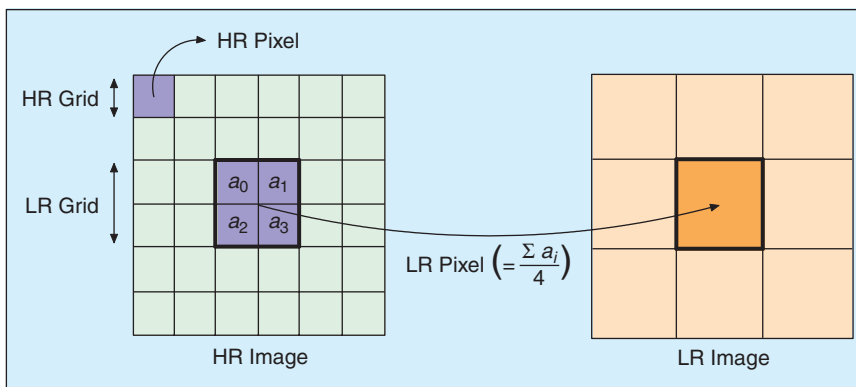
▲ 5. Low-resolution sensor PSF.

zero-order hold or bilinear interpolation methods have been used in many literatures.

Blurring may be caused by an optical system (e.g., out of focus, diffraction limit, aberration, etc.), relative motion between the imaging system and the original scene, and the point spread function (PSF) of the LR sensor. It can be modeled as linear space invariant (LSI) or linear space variant (LSV), and its effects on HR images are represented by the matrix $\mathbf{B}_k$. In single image restoration applications, the optical or motion blur is usually considered. In the SR image reconstruction, however, the finiteness of a physical dimension in LR sensors is an important factor of blur. This LR sensor PSF is usually modeled as a spatial averaging operator as shown in Figure 5. In the use of SR reconstruction methods, the characteristics of the blur are assumed to be known. However, if it is difficult to obtain this information, blur identification should be incorporated into the reconstruction procedure.

The subsampling matrix **D** generates aliased LR images from the warped and blurred HR image. Although the size of LR images is the same here, in more general cases, we can address the different size of LR images by using a different subsampling matrix (e.g., $\mathbf{D}_k$). Although the blurring acts more or less as an anti-aliasing filter, in SR image reconstruction, it is assumed that aliasing is always present in LR images.

A slightly different LR image acquisition model can be derived by discretizing a continuous warped, blurred scene [24]-[28]. In this case, the observation model must include the fractional pixels at the border of the blur support. Although there are some different considerations between this model and the one in (1), these models can be unified in a simple matirx-vector form since the LR pixels are defined as a weighted sum of the related HR pixels with additive noise [18]. Therefore, we can express these models without loss of generality as follows:

$$\mathbf{y}_k = \mathbf{W}_k \mathbf{x} + \mathbf{n}_k, \quad \text{for} \quad k = 1, ..., p, \tag{2}$$

where matrix $\mathbf{W}_k$ of size $(N_1 N_2)^2 \times L_1 N_1 L_2 N_2$ represents, via blurring, motion, and subsampling, the contribution of HR pixels in **x** to the LR pixels in $\mathbf{y}_k$. Based on the observation model in (2), the aim of the SR image reconstruction is to estimate the HR image **x** from the LR images $\mathbf{y}_k$ for $k = 1, ..., p$.

Most of the SR image reconstruction methods proposed in the literature consist of the three stages illustrated in Figure 6: registration, interpolation, and restoration (i.e., inverse procedure). These steps can be implemented separately or simultaneously according to the reconstruction methods adopted. The estimation of motion information is referred to as registration, and it is extensively studied in various fields of image processing [67]-[70]. In the

registration stage, the relative shifts between LR images compared to the reference LR image are estimated with fractional pixel accuracy. Obviously, accurate subpixel motion estimation is a very important factor in the success of the SR image reconstruction algorithm. Since the shifts between LR images are arbitrary, the registered HR image will not always match up to a uniformly spaced HR grid. Thus, nonuniform interpolation is necessary to obtain a uniformly spaced HR image from a nonuniformly spaced composite of LR images. Finally, image restoration is applied to the upsampled image to remove blurring and noise.

The differences among the several proposed works are subject to what type of reconstruction method is employed, which observation model is assumed, in which particular domain (spatial or frequency) the algorithm is applied, what kind of methods is used to capture LR images, and so on. The technical report by Borman and Stevenson [2] provides a comprehensive and complete overview on the SR image reconstruction algorithms until around 1998, and a brief overview of the SR techniques appears in [3] and [4].

Based on the observation model in (2), existing SR algorithms are reviewed in the following sections. We first present a nonuniform interpolation approach that conveys an intuitive comprehension of the SR image reconstruction. Then, we explain a frequency domain approach that is helpful to see how to exploit the aliasing relationship between LR images. Next, we present deterministic and stochastic regularization approaches, the projection onto convex sets (POCS) approach, as well as other approaches. Finally, we discuss advanced issues to improve the performance of the SR algorithm.

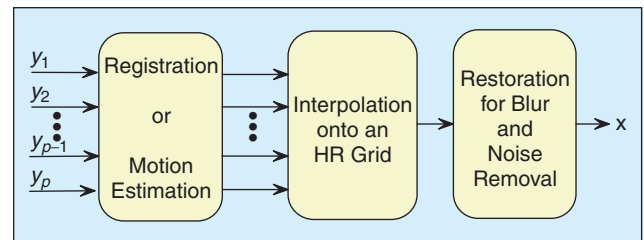## SR Image Reconstruction Algorithms

Nonuniform Interpolation Approach

This approach is the most intuitive method for SR image reconstruction. The three stages presented in Figure 6 are performed successively in this approach: i) estimation of relative motion, i.e., registration (if the motion information is not known), ii) nonuniform interpolation to produce an improved resolution image, and iii) deblurring process (depending on the observation model). The pictorial example is shown in Figure 7. With the relative motion information estimated, the HR image on nonuniformly spaced sampling points is obtained. Then, the direct or iterative reconstruction procedure is followed to produce uniformly spaced sampling points [71]-[74]. Once an HR image is obtained by nonuniform interpolation, we address the restoration problem to remove blurring and noise. Restoration can be performed by applying any

deconvolution method that considers the presence of noise.

The reconstruction results of this approach appear in Figure 8. In this simulation, four LR images are generated by a decimation factor of two in both the horizontal and vertical directions from the 256×256 HR image. Only sensor blur is considered here, and a 20-dB Gaussian noise is added to these LR images. In Figure 8, part (a) shows the image interpolated by the nearest neighborhood method from one LR observation, and part (b) is the image produced by bilinear interpolation; a nonuniformly interpolated image from four LR images appears in part (c), and a deblurred image using the Wiener restoration filter from part (c) is shown in part (d). As shown in Figure 8, significant improvement is observed in parts (c) and (d) when viewed in comparison with parts (a) and (b).

Ur and Gross [5] performed a nonuniform interpolation of an ensemble of spatially shifted LR images by utilizing the generalized multichannel sampling theorem of Papoulis [73] and Brown [74]. The interpolation is followed by a deblurring process, and the relative shifts are assumed to be known precisely here. Komatsu et al. [1] presented a scheme to acquire an improved resolution image by applying the Landweber algorithm [75] from multiple images taken simultaneously with multiple cameras. They employ the block-matching technique to measure relative shifts. If the cameras have the same aperture, however, it imposes severe limitations both in their arrangement and in the configuration of the scene. This difficulty was overcome by using multiple cameras with different apertures [6]. Hardie et al. developed a technique for real-time infrared image registration and SR reconstruction [7]. They utilized a gradient-based


▲ 6. Scheme for super resolution.
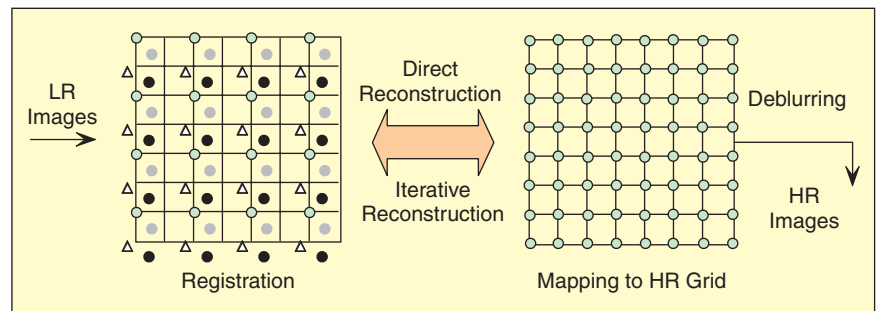
▲ 7. Registration-interpolation-based reconstruction.

registration algorithm for estimating the shifts between the acquired frames and presented a weighted nearest neighbor interpolation approach. Finally, Wiener filtering is applied to reduce effects of blurring and noise caused by the system. Shah and Zakhor proposed an SR color video enhancement algorithm using the Landweber algorithm [8]. They also consider the inaccuracy of the registration algorithm by finding a set of candidate motion estimates instead of a single motion vector for each pixel. They use both luminance and chrominance information to estimate the motion field. Nguyen and Milanfar [9] proposed an efficient wavelet-based SR reconstruction algorithm. They exploit the interlacing structure of the sampling grid in SR and derive a computationally efficient wavelet interpolation for interlaced two-dimensional (2-D) data.

The advantage of the nonuniform interpolation approach is that it takes relatively low computational load and makes real-time applications possible. However, in this approach, degradation models are limited (they are only applicable when the blur and the noise characteristics are the same for all LR images). Additionally, the optimality of the whole reconstruction algorithm is not guaranteed, since the restoration step ignores the errors that occur in the interpolation stage.
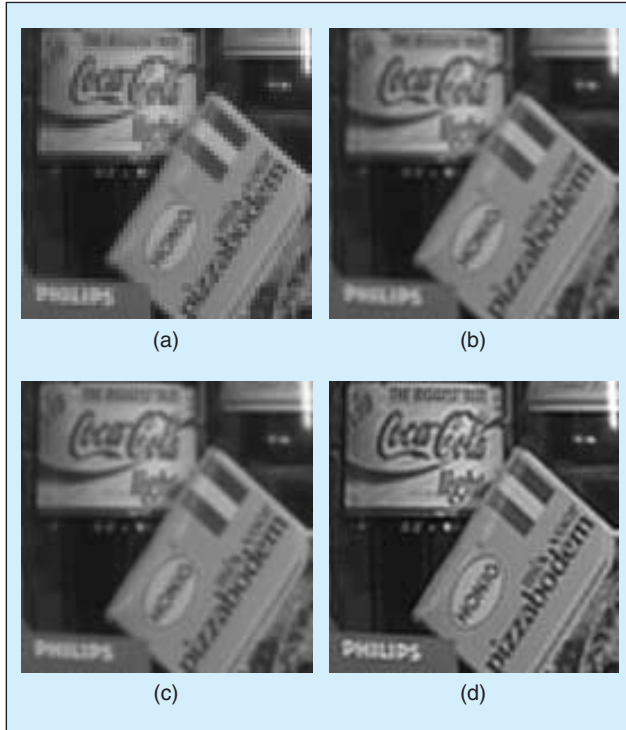
▲ 8. Nonuniform interpolation SR reconstruction results by (a) nearest neighbor interpolation, (b) bilinear interpolation, (c) nonuniform interpolation using four LR images, and (d) deblurring part (c).
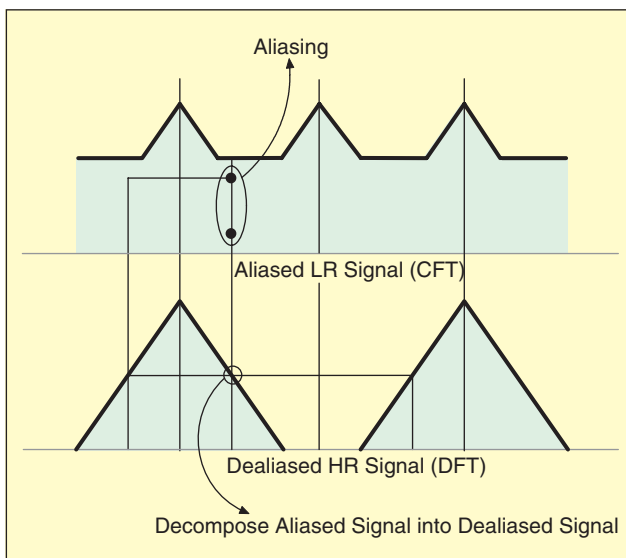
Frequency Domain Approach

The frequency domain approach makes explicit use of the aliasing that exists in each LR image to reconstruct an HR image. Tsai and Huang [10] first derived a system equation that describes the relationship between LR images and a desired HR image by using the relative motion between LR images. The frequency domain approach is based on the following three principles: i) the shifting property of the Fourier transform, ii) the aliasing relationship between the continuous Fourier transform (CFT) of an original HR image and the discrete Fourier transform (DFT) of observed LR images, iii) and the assumption that an original HR image is bandlimited. These properties make it possible to formulate the system equation relating the aliased DFT coefficients of the observed LR images to a sample of the CFT of an unknown image. For example, let us assume that there are two 1-D LR signals sampled below the Nyquist sampling rate. From the above three principles, the aliased LR signals can be decomposed into the unaliased HR signal as shown in Figure 9.

Let $x(t_1, t_2)$ denote a continuous HR image and $X(w_1, w_2)$ be its CFT. The global translations, which are the only motion considered in the frequency domain approach, yield the kth shifted image of $x_k(t_1, t_2) = x(t_1 + \delta_{k1}, t_2 + \delta_{k2})$, where δ_{k1} and δ_{k2} are arbitrary but known values, and $k = 1, 2, .., p$. By the shifting property of the CFT, the CFT of the shifted image, $X_k(w_1, w_2)$, can be written as

$$X_k(w_1, w_2) = \exp\left[j2\pi\left(\delta_{k1} w_1 + \delta_{k2} w_2\right)\right] X(w_1, w_2). \quad (3)$$

The shifted image $x_k(t_1, t_2)$ is sampled with the sampling period T_1 and T_2 to generate the observed LR image $y_k[n_1, n_2]$. From the aliasing relationship and the assumption of bandlimitedness of $X(w_1, w_2)$ ($|X(w_1, w_2)| = 0$ for $|w_1| \geq (L_1 \pi / T_1)$, $|w_2| \geq (L_2 \pi / T_2)$), the relationship between the CFT of the HR image and the DFT of the kth observed LR image can be written as [76]

▲ 9. Aliasing relationship between LR image and HR image.

$$\Upsilon_k[\Omega_1,\Omega_2] = \frac{1}{T_1 T_2} \sum_{n_1=0}^{L_1-1} \sum_{n_2=0}^{L_2-1} X_k$$
$$\times \left(\frac{2\pi}{T_1}\left(\frac{\Omega_1}{N_1}+n_1\right), \frac{2\pi}{T_2}\left(\frac{\Omega_2}{N_2}+n_2\right) \right).$$

$$(4)$$

By using lexicographic ordering for the indices n_1, n_2 on the right-hand side and k on the left-hand side, a matrix vector form is obtained as:

$$\mathbf{Y} = \Phi \mathbf{X}, \qquad\qquad (5)$$

where $\mathbf{Y}$ is a $p \times 1$ column vector with the kth element of the DFT coefficients of $y_k[n_1,n_2]$, $\mathbf{X}$ is a $L_1 L_2 \times 1$ column vector with the samples of the unknown CFT of $x(t_1,t_2)$, and Φ is a $p \times L_1 L_2$ matrix which relates the DFT of the observed LR images to samples of the continuous HR image. Therefore, the reconstruction of a desired HR image requires us to determine Φ and solve this inverse problem.

An extension of this approach for a blurred and noisy image was provided by Kim et al. [11], resulting in a weighted least squares formulation. In their approach, it is assumed that all LR images have the same blur and the same noise characteristics. This method was further refined by Kim and Su [12] to consider different blurs for each LR image. Here, the Tikhonov regularization method is adopted to overcome the ill-posed problem resulting from blur operator. Bose et al. [13] proposed the recursive total least squares method for SR reconstruction to reduce effects of registration errors (errors in Φ). A discrete cosine transform (DCT)-based method was proposed by Rhee and Kang [14]. They reduce memory requirements and computational costs by using DCT instead of DFT. They also apply multichannel adaptive regularization parameters to overcome ill-posedness such as underdetermined cases or insufficient motion information cases.

Theoretical simplicity is a major advantage of the frequency domain approach. That is, the relationship between LR images and the HR image is clearly demonstrated in the frequency domain. The frequency method is also convenient for parallel implementation capable of reducing hardware complexity. However, the observation model is restricted to only global translational motion and LSI blur. Due to the lack of data correlation in the frequency domain, it is also difficult to apply the spatial domain a priori knowledge for regularization.

Regularized SR Reconstruction Approach
Generally, the SR image reconstruction approach is an ill-posed problem because of an insufficient number of LR images and ill-conditioned blur operators. Procedures adopted to stabilize the inversion of ill-posed problem are called regularization. In this section, we present deterministic and stochastic regularization approaches for SR image reconstruction. Typically, constrained least

The basic premise for increasing the spatial resolution in SR techniques is the availability of multiple LR images captured from the same scene.

squares (CLS) and maximum a posteriori (MAP) SR image reconstruction methods are introduced.

Deterministic Approach
With estimates of the registration parameters, the observation model in (2) can be completely specified. The deterministic regularized SR approach solves the inverse problem in (2) by using the prior information about the solution which can be used to make the problem well posed. For example, CLS can be formulated by choosing an $\mathbf{x}$ to minimize the Lagrangian [63]

$$\left[\sum_{k=1}^{p} \left\| \mathbf{y}_k - \mathbf{W}_k \mathbf{x} \right\|^2 + \alpha \left\| \mathbf{C}\mathbf{x} \right\|^2 \right],$$

$$(6)$$

where the operator $\mathbf{C}$ is generally a high-pass filter, and $\|\cdot\|$ represents a l_2-norm. In (6), a priori knowledge concerning a desirable solution is represented by a smoothness constraint, suggesting that most images are naturally smooth with limited high-frequency activity, and therefore it is appropriate to minimize the amount of high-pass energy in the restored image. In (6), α represents the Lagrange multiplier, commonly referred to as the regularization parameter, that controls the tradeoff between fidelity to the data (as expressed by $\sum_{k=1}^{p} \left\| \mathbf{y}_k - \mathbf{W}_k \mathbf{x} \right\|^2$) and smoothness of the solution (as expressed by $\|\mathbf{C}\mathbf{x}\|^2$). The Larger values of α will generally lead to a smoother solution. This is useful when only a small number of LR images are available (the problem is underdetermined) or the fidelity of the observed data is low due to registration error and noise. On the other hand, if a large number of LR images are available and the amount of noise is small, small α will lead to a good solution. The cost functional in (6) is convex and differentiable with the use of a quadratic regularization term. Therefore, we can find a unique estimate image $\hat{\mathbf{x}}$ which minimizes the cost functional in (6). One of the most basic deterministic iterative techniques considers solving

$$\left[\sum_{k=1}^{p} \mathbf{W}_k^{\mathrm{T}} \mathbf{W}_k + \alpha \mathbf{C}^{\mathrm{T}} \mathbf{C} \right] \hat{\mathbf{x}} = \sum_{k=1}^{p} \mathbf{W}_k^{\mathrm{T}} \mathbf{y}_k,$$

$$(7)$$

and this leads to the following iteration for $\hat{\mathbf{x}}$:

$$\hat{\mathbf{x}}^{n+1} = \hat{\mathbf{x}}^n + \beta \left[\sum_{k=1}^{p} \mathbf{W}_k^{\mathrm{T}} (\mathbf{y}_k - \mathbf{W}_k \hat{\mathbf{x}}^n) - \alpha \mathbf{C}^{\mathrm{T}} \mathbf{C} \hat{\mathbf{x}}^n \right],$$

$$(8)$$

where β represents the convergence parameter and $\mathbf{W}_k^T$ contains an upsampling operator and a type of blur and warping operator.

Katsaggelos et al. [15], [16] proposed a multichannel regularized SR approach in which regularization functional is used to calculate the regularization parameter without any prior knowledge at each iteration step. Later, Kang formulated the generalized multichannel deconvoultion method including the multichannel regularized SR approach [17]. The SR reconstruction method obtained by minimizing a regularized cost functional was proposed by Hardie et al. [18]. They define an observation model that incorporates knowledge of the optical system and the detector array (sensor PSF). They used an iterative gradient-based registration algorithm and considered both gradient descent and conjugate-gradient optimization procedures to minimize the cost functional. Bose et al. [19] pointed to the important role of the regularization parameter and a proposed CLS SR reconstruction which generates the optimum value of the regularization parameter, using the L-curve method [77].

Stochastic Approach

Stochastic SR image reconstruction, typically a Bayesian approach, provides a flexible and convenient way to model a priori knowledge concerning the solution.

Bayesian estimation methods are used when the a posteriori probability density function (PDF) of the original

▲ 10. Regularized SR reconstruction results by (a) nearest neighbor interpolation, (b) CLS with small regularization parameter, (c) CLS with large regularization parameter, and (d) MAP with edge-preserving prior.

image can be established. The MAP estimator of $\mathbf{x}$ maximizes the a posteriori PDF $P(\mathbf{x}|\mathbf{y}_k)$ with respect to $\mathbf{x}$

$$\mathbf{x} = \arg\max P(\mathbf{x}|\mathbf{y}_1,\mathbf{y}_2,\ldots,\mathbf{y}_p). \tag{9}$$

Taking the logarithmic function and applying Bayes' theorem to the conditional probability, the MAP optimization problem can be expressed as

$$\mathbf{x} = \arg\max\left\{\ln P(\mathbf{y}_1,\mathbf{y}_2,\ldots,\mathbf{y}_p|\mathbf{x}) + \ln P(\mathbf{x})\right\}. \tag{10}$$

Here, both the a priori image model $P(\mathbf{x})$ and the conditional density $P(\mathbf{y}_1,\mathbf{y}_2,\ldots,\mathbf{y}_p|\mathbf{x})$ will be defined by a priori knowledge concerning the HR image $\mathbf{x}$ and the statistical information of noise. Since MAP optimization in (10) includes a priori constraints (prior knowledge represented by $P(\mathbf{x})$) essentially, it provides regularized (stable) SR estimates effectively. Bayesian estimation distinguishes between possible solutions by utilizing a priori image model, and Markov random field (MRF) priors that provide a powerful method for image prior modeling are often adopted. Using the MRF prior, $P(\mathbf{x})$ is described by a Gibbs prior whose probability density is defined as

$$P(\mathbf{X} = \mathbf{x}) = \frac{1}{Z}\exp\{-U(\mathbf{x})\} = \frac{1}{Z}\exp\left\{-\sum_{c\in S}\varphi_c(\mathbf{x})\right\}, \tag{11}$$

where Z is simply a normalizing constant, $U(\mathbf{x})$ is called an energy function, $\varphi_c(\mathbf{x})$ is a potential function that depends only on the pixel values located within clique c, and S denotes the set of cliques. By defining $\varphi_c(\mathbf{x})$ as a function of the derivative of the image, $U(\mathbf{x})$ measures the cost caused by the irregularities of the solution. Commonly, an image is assumed to be globally smooth, which is incorporated into the estimation problem through a Gaussian prior.

A major advantage of the Bayesian framework is the use of an edge-preserving image prior model. With the Gaussian prior, the potential function takes the quadratic form $\varphi_c(\mathbf{x}) = (D^{(n)}\mathbf{x})^2$ where $D^{(n)}$ is an nth order difference. Though the quadratic potential function makes the algorithm linear, it penalizes the high-frequency components severely. As a result, the solution becomes oversmoothed. However, if we model a potential function which less penalizes the large difference in $\mathbf{x}$, we can obtain an edge-preserving HR image.

If the error between frames is assumed to be independent and noise is assumed to be an independent identically distributed (i.i.d) zero mean Gaussian distribution, the optimization problem can be expressed more compactly as

$$\hat{\mathbf{x}} = \arg\min\left[\sum_{k=1}^{p}\left\|\mathbf{y} - \mathbf{W}_k\hat{\mathbf{x}}\right\|^2 + \alpha\sum_{c\in S}\varphi_c(\mathbf{x})\right], \tag{12}$$

where α is the regularization parameter. Finally, it can be shown that the estimate defined in (6) is equal to a MAP estimate if we use the Gaussian prior in (12).
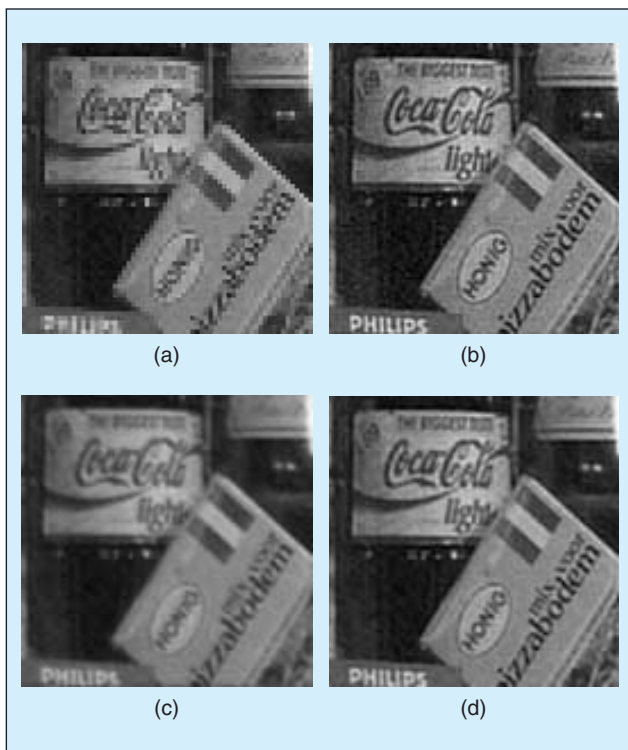
A maximum likelihood (ML) estimation has also been applied to the SR reconstruction. The ML estimation is a special case of MAP estimation with no prior term. Due to the ill-posed nature of SR inverse problems, however, MAP estimation is usually used in preference to ML.

The simulation results of regularized SR methods are shown in Figure 10. In these simulations, the original 256×256 shop image is shifted with one of the subpixel shifts {(0,0), (0,0.5), (0.5,0), (0.5,0.5)} and decimated by a factor of two in both the horizontal and vertical directions. Here, only sensor blur is considered and a 20 dB Gaussian noise is added to these LR images. Figure 10(a) is a nearest neighborhood interpolated image from one of the LR images. CLS SR results using a small regularization parameter and a large regularization parameter appear in Figure 10(b) and(c), respectively. In fact, these estimates can be considered as those of MAP reconstruction with Gaussian prior. Figure 10(d) shows the SR result with an edge-preserving Huber-Markov prior [21]. By far, the poorest reconstruction is the nearest neighbor interpolated image. This poor performance is easily attributed to the independent processing of the LR observations, and it is apparent throughout Figure 10(a). Compared to this method, CLS SR results in Figure 10(b) and (c) show significant improvements by retaining detailed information. We observe that these improvements are further obtained by using the edge-preserving prior as shown in Figure 10(d).

Tom and Katsaggelos [20] proposed the ML SR image estimation problem to estimate the subpixel shifts, the noise variances of each image, and the HR image simultaneously. The proposed ML estimation problem is solved by the expectation-maximization (EM) algorithm. The SR reconstruction from an LR video sequence using the MAP technique was proposed by Schultz and Stevenson [21]. They proposed a discontinuity preserving the MAP reconstruction method using the Huber-Markov Gibbs prior model, resulting in a constrained optimization problem with a unique minimum. Here, they used the modified hierarchical block matching algorithm to estimate the subpixel displacement vectors. They also consider independent object motion and inaccurate motion estimates that are modeled by Gaussian noise. A MAP framework for the joint estimation of image registration parameters and the HR image was presented by Hardie et al. in [22]. The registration parameters, horizontal and vertical shifts in this case, are iteratively updated along with the HR image in a cyclic optimization procedure. Cheeseman et al. applied the Bayesian estimation with a Gaussian prior model to the problem of integrating multiple satellite images observed by the Viking orbiter [23].

Robustness and flexibility in modeling noise characteristics and a priori knowledge about the solution are the major advantage of the stochastic SR approach. Assuming that the noise process is white Gaussian, a MAP estimation with convex energy functions in the priors en-

Registration is a very important step to the success of the SR image reconstruction.

sures the uniqueness of the solution. Therefore, efficient gradient descent methods can be used to estimate the HR image. It is also possible to estimate the motion information and the HR image simultaneously.

Projection onto Convex Sets Approach

The POCS method describes an alternative iterative approach to incorporating prior knowledge about the solution into the reconstruction process. With the estimates of registration parameters, this algorithm simultaneously solves the restoration and interpolation problem to estimate the SR image.

The POCS formulation of the SR reconstruction was first suggested by Stark and Oskoui [24]. Their method was extended by Tekalp et al. to include observation noise [25]. According to the method of POCS [63], incorporating a priori knowledge into the solution can be interpreted as restricting the solution to be a member of a closed convex set C_i that are defined as a set of vectors which satisfy a particular property. If the constraint sets have a nonempty intersection, then a solution that belongs to the intersection set $C_s = \cap_{i=1}^{m} C_i$, which is also a convex set, can be found by alternating projections onto these convex sets. Indeed, any solution in the intersection set is consistent with the a priori constraints and therefore it is a feasible solution. The method of POCS can be applied to find a vector which belongs in the intersection by the recursion

$$x^{n+1} = P_m P_{m-1} \cdots P_2 P_1 x^n, \qquad (13)$$

where x^0 is an arbitrary starting point, and P_i is the projection operator which projects an arbitrary signal x onto the closed, convex sets, $C_i (i = 1, 2, ..., m)$. Although this may not be a trivial task, it is, in general, much easier than finding P_s, i.e., the projector that projects onto the solution set C_s in one step [24].

Assuming that the motion information is accurate, a data consistency constraint set based on the observation model in (2) is represented for each pixel within the LR images $y_k[m_1, m_2]$ [25], [26]:

$$C_D^k[m_1, m_2] = \left\{ x[n_1, n_2] : \left| r^{(x)}[m_1, m_2] \right| \le \delta_k[m_1, m_2] \right\},$$
$$(14)$$

where

$$r^{(x)}[m_1, m_2] = y_k[m_1, m_2]$$
$$- \sum_{n_1, n_2} x[n_1, n_2] W_k[m_1, m_2; n_1, n_2], \qquad (15)$$

and $\delta_k[m_1, m_2]$ is a bound reflecting the statistical confidence, with which the actual image is a member of the set $C_D^k[m_1, m_2]$ [26]. Since the bound $\delta_k[m_1, m_2]$ is determined from the statistics of the noise process, the ideal solution is a member of the set within a certain statistical confidence. Furthermore, the POCS solution will be able to model space- and time-varying white noise processes. The projection of an arbitrary $x[n_1, n_2]$ onto $C_D^k[m_1, m_2]$ can be defined as [25], [78]

$$x^{(n+1)}[n_1, n_2] = x^{(n)}[n_1, n_2]$$

$$+ \begin{cases} \dfrac{(r^{(x)}[m_1, m_2] - \delta_k[m_1, m_2]) \cdot W_k[m_1, m_2, n_1, n_2]}{\sum_{p,q} W_k^2[m_1, m_2, p, q]}, \\ \quad r^{(x)}[m_1, m_2] > \delta_k[m_1, m_2] \\ 0, \quad |r^{(x)}[m_1, m_2]| \leq \delta_k[m_1, m_2] \\ \dfrac{(r^{(x)}[n_1, n_2] + \delta_k[n_1, n_2]) \cdot W_k[m_1, m_2, n_1, n_2]}{\sum_{p,q} W_k^2[m_1, m_2, p, q]}, \\ \quad r^{(x)}[m_1, m_2] < -\delta_k[m_1, m_2]. \end{cases}$$

$$(16)$$

Additional constraints such as amplitude constraint after (16) can be utilized to improve the results [24].

Reconstruction results by POCS using data constraint and amplitude constraint appear in Figure 11. In this simulation, four LR images are generated by a decimation factor of two in both the horizontal and vertical directions from the 256×256 HR image, and a 20 dB Gaussian noise is added to these LR images. In this simulation, sensor blur is only considered. Figure 11(a) shows a bilinearly interpolated image of one of the LR observations, and parts (b)-(d) are the reconstruction results after 10, 30, and 50 iterations. Comparing the result by bilinear interpolation in Figure 11(a), we observe that the improvement of the results by POCS SR reconstruction is evident.

Patti et al. [26] developed a POCS SR technique to consider space varying blur, nonzero aperture time, nonzero physical dimension of each individual sensor element, sensor noise, and arbitrary sampling lattices. Tekalp et al. then extended the technique to the case of multiple moving objects in the scene by introducing the concept of a validity map and/or a segmentation map [27]. The validity map allows robust reconstruction in the presence of registration errors, and the segmentation map enables object-based SR reconstruction. In [28], a POCS-based SR reconstruction method where a continuous image formation model is improved to allow for higher order interpolation methods was proposed by Patti and Altunbasak. In this work, they assume a continuous scene within an HR sensor area is not constant. They also modify the constraint set to reduce the ringing artifact in the vicinity of edges. A set theoretic regularization approach similar to POCS formulation was investigated by Tom and Katsaggelos [29]. Using ellipsoidal constraint sets, they find the SR estimate which is the centroid of a bounding ellipsoid (set intersection).

The advantage of POCS is that it is simple, and it utilizes the powerful spatial domain observation model. It also allows a convenient inclusion of a priori information. These methods have the disadvantages of nonuniqueness of solution, slow convergence, and a high computational cost.

ML-POCS Hybrid Reconstruction Approach

The ML-POCS hybrid reconstruction approach finds SR estimates by minimizing the ML (or MAP) cost functional while constraining the solution within certain sets.

Earlier efforts for this formulation are found in the work by Schultz and Stevenson [21] where MAP optimization is performed while projections-based constraint is also utilized. Here, the constraint set ensures that the down-sampled version of the HR image matched the reference frame of the LR sequence. Elad and Feuer [30] proposed a general hybrid SR image reconstruction algorithm which combines the benefits of the stochastic approaches and the POCS approach. The simplicity of the ML (or MAP) and the nonellipsoid constraints used in POCS are utilized simultaneously by defining a new convex optimization problem as follows:

$$\min \varepsilon^2 = \left\{ [\mathbf{y}_k - \mathbf{W}_k \mathbf{x}]^T \mathbf{R}_n^{-1} [\mathbf{y}_k - \mathbf{W}_k \mathbf{x}] + \alpha [\mathbf{S}\mathbf{x}]^T \mathbf{V}[\mathbf{S}\mathbf{x}] \right\},$$

$$(17)$$

subject to
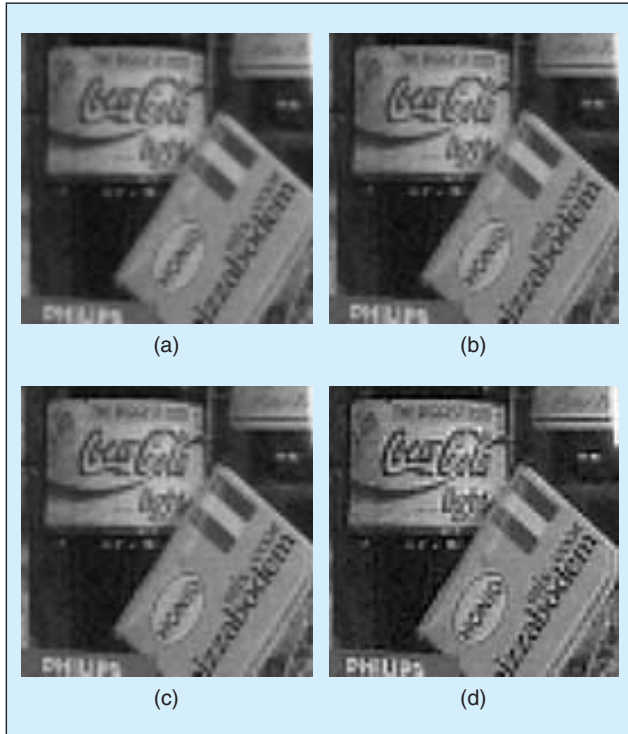
▲ 11. POCS SR results (a) by bilinear interpolation and by POCS after (b) 10 iterations, (c) 30 iterations, and (d) 50 iterations.

$$\{\mathbf{x} \in C_k, 1 \le k \le M\} \qquad (18)$$

where $\mathbf{R}_n$ is the autocorrelation matrix of noise, $\mathbf{S}$ is the Laplacian operator, $\mathbf{V}$ is the weighting matrix to control the smoothing strength at each pixel, and C_k represents the additional constraint.

The advantage of the hybrid approach is that all a priori knowledge is effectively combined, and it ensures a single optimal solution in contrast to the POCS approach.

Other SR Reconstruction Approaches

Iterative Back-Projection Approach
Irani and Peleg [31] formulated the iterative back-projection (IBP) SR reconstruction approach that is similar to the back projection used in tomography. In this approach, the HR image is estimated by back projecting the error (difference) between simulated LR images via imaging blur and the observed LR images. This process is repeated iteratively to minimize the energy of the error. The IBP scheme to estimate the HR image is expressed by
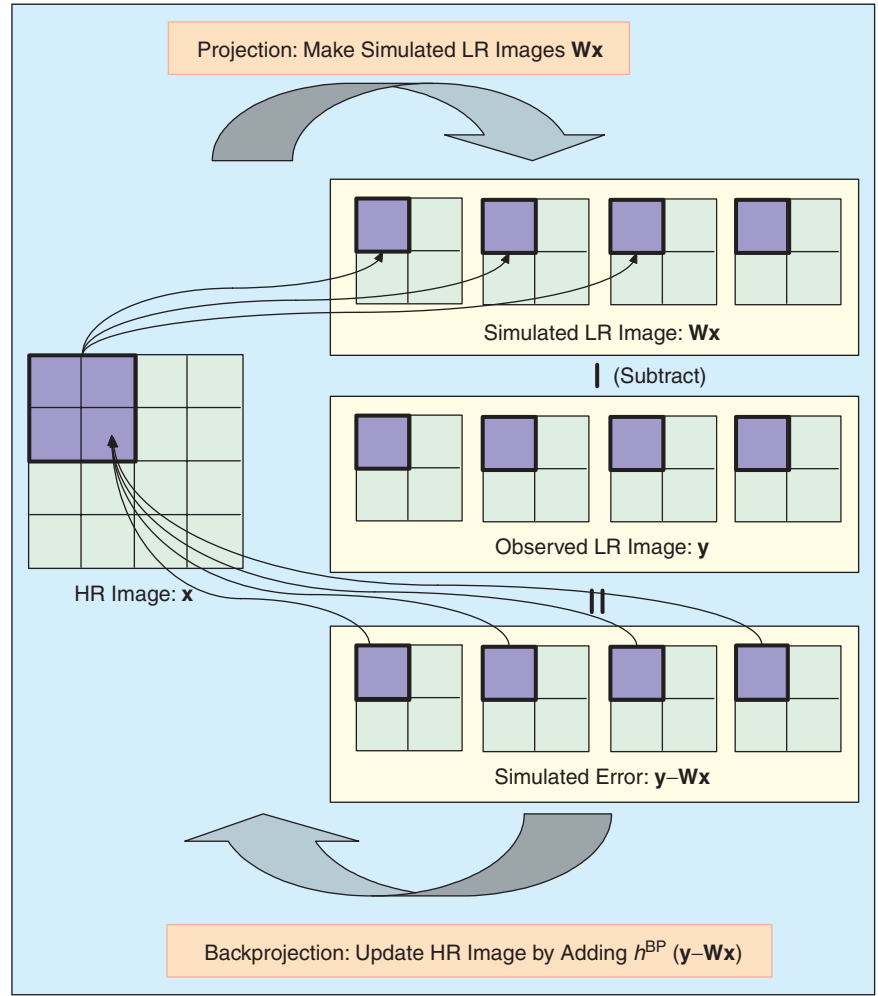
▲ 12. A pictorial example of IBP method.

$$\hat{x}^{n+1}[n_1, n_2] = \hat{x}^{n}[n_1, n_2]$$
$$+ \sum_{m_1, m_2 \in \Upsilon_k^{m_1, n_1}} \left(y_k[m_1, m_2] - \hat{y}_k^{n}[m_1, m_2] \right)$$
$$\times h^{\mathrm{BP}}[m_1, m_2; n_1, n_2] \qquad (19)$$

where $\hat{y}_k^{n} (= W_k \hat{x}^{n})$ are simulated LR images from the approximation of x after n iteration, $\Upsilon_k^{m_1, n_1}$ denotes the set $\{m_1, m_2 \in y_k | m_1, m_2 \text{ is influenced by } n_1, n_2, \text{ where } n_1, n_2 \in x\}$ and $h^{\mathrm{BP}}(m_1, m_2; n_1, n_2)$ is a back-projection kernel that determines the contribution of the error $(y_k[m_1, m_2] - \hat{y}_k^{n}[m_1, m_2])$ to $\hat{x}^{n}[n_1, n_2]$ properly. The scheme for IBP is illustrated in Figure 12. Unlike imaging blur, h^{BP} can be chosen arbitrarily. In [31], it is pointed out that the choice of h^{BP} affects the characteristics of the solution when there are possible solutions. Therefore, h^{BP} may be utilized as an additional constraint which represents the desired property of the solution. Mann and Picard [32] extended this approach by applying a perspective motion model in the image acquisition process. Later, Irani and Peleg [33] modified the IBP to consider a more general motion model.

The advantage of IBP is that it is understood intuitively and easily. However, this method has no unique solution due to the ill-posed nature of the inverse problem, and it has some difficulty in choosing the h^{BP}. In contrast to the POCS and regularized approach, it is difficult to apply a priori constraints.

Adaptive Filtering Approach
Elad and Feuer [34] proposed an SR image reconstruction algorithm based on adaptive filtering theory applied in time axis. They modified notation in the observation model to accommodate for its dependence on time and suggested least squares (LS) estimators based on a pseudo-RLS or R-LMS algorithm. The steepest descent (SD) and normalized SD are applied to estimate the HR image at each time iteratively, and the LMS algorithm is derived from the SD algorithm. As a result, the HR image at each time is calculated without computational complexity of a direct matrix inversion. This approach is shown to be capable of treating any chosen output resolution, linear time and space variant blur, and motion flow [34], which makes the progressive estimation of HR image sequence possible. Following this research, they rederive the R-SD and R-LMS algorithm as an approximation of the Kalman filter

SR image reconstruction is one of the most spotlighted research areas, because it can overcome the inherent resolution limitation of the imaging system and improve the performance of most digital image processing applications.

[35]. Here, convergence analysis and computational complexity issues of these algorithms were also discussed.

Motionless SR Reconstruction Approach

The SR reconstruction algorithms presented so far require relative subpixel motions between the observed images. However, it is shown that SR reconstruction is also possible from differently blurred images without relative motion [30], [37]. Elad and Feuer [30] demonstrated that the motionless SR image reconstruction without a regularization term is possible if the following necessary condition is satisfied:

$$L^2 \leq \min\left\{(2m+1)^2 - 2, p\right\}, \qquad (20)$$

where $(2m+1)\times(2m+1)$ is the size of the blurring kernel, and $L_1 = L_2 = L$. Hence, although more numbers of blurred observations of a scene do not provide any additional information, it is possible to achieve SR with these blurred samples, provided (20) is satisfied. Note that one can recover the HR image with much fewer LR images if a regularization is incorporated to the reconstruction procedure. Rajan and Chaudhuri [37], [38] proposed a similar motionless SR technique for intensity and depth maps using an MRF model of the image field. There have been other motionless attempts to SR imaging [39], [40]. Rajan and Chaudhuri [39] presented the SR method using photometric cues, and the SR technique using zoom as a cue is proposed by Joshi and Chaudhuri [40].

Advanced Issues in SR

In the previous sections, we reviewed the existing SR reconstruction methods which are frequently employed. In this section, we illustrate the advanced issues which are important open problems within the SR area.

SR Considering Registration Error

Registration is a very important step to the success of the SR image reconstruction as mentioned earlier. Therefore, accurate registration methods, based on robust motion models including multiple object motion, occlusions, transparency, etc., should be needed [3]. However, when we cannot ensure the performance of the registration algorithms in certain environments, the error caused by an inaccurate registration should be considered in the reconstruction procedure. Although most SR algorithms implicitly model the registration error as an additive Gaussian noise, more sophisticated models for this error are needed.

Bose et al. [41], [42] considered the error generated by inaccurate registration in the system matrix $\mathbf{W}_k$ and proposed the total least squares method to minimize the error. This method is shown to be useful for improving the solution accuracy when errors exist not only in the recording process but also in the measurement matrix. Ng and Bose analyzed displacement errors on the convergence rate of the iteration used in solving the transform-based preconditioned system [43]. Here, LR images are acquired from multiple cameras which are shifted from each other by a known subpixel displacement. In this environment, small perturbations around the ideal subpixel locations of the sensing elements are always produced due to imperfect fabrication, and therefore the registration error is generated along the boundary of blur support. From this unstable blur matrix, they proved the linear convergence of the conjugate gradient method.

Another approach to minimize the effect of the registration error is based on channel adaptive regularization [44]-[46]. The basic concept of channel adaptive regularization is that LR images with a large amount of registration error should be less contributed to the estimate of the HR image than reliable LR images. Kang et al. [44] assumed that the degree of registration error is different in each channel (LR image) and applied the regularization functionals [79] to adaptively control the effect of registration error in each channel. Kang et al. [45] showed that the tendency of high-frequency components in the HR image is closely related to the registration error and used the directional smoothing constraint. Here, the registration error is modeled as Gaussian noise which has a different variance according to the registration axes, and channel adaptive regularization is performed with a directional smoothing constraint. Kang et al. [46] extended these works based on a set-theoretic approach. They proposed the regularization functional that is performed on the data consistency term. As a result, the minimization functional is defined as $\sum_{k=1}^{p} \lambda_k(\mathbf{x})\|\mathbf{y}_k - \mathbf{W}_k\mathbf{x}\|^2 + \|\mathbf{C}\mathbf{x}\|^2$. They proposed that the desirable properties of the regularization functional $\lambda_k(\mathbf{x})$ to reduce the effects of error in the reconstruction procedure as follows:

▲ $\lambda_k(\mathbf{x})$ is inversely proportional to $\|\mathbf{y}_k - \mathbf{W}_k\mathbf{x}\|^2$

▲ $\lambda_k(\mathbf{x})$ is proportional to $\|\mathbf{C}\mathbf{x}\|^2$

▲ $\lambda_k(\mathbf{x})$ is larger than zero

▲ $\lambda_k(\mathbf{x})$ considers the influence of the cross channel.

With this channel-adaptive regularization, the improvement in the SR reconstruction appears in Figure 13. In the simulation, each 128×128 observation is constructed with one of the subpixel shifts $\{(0,0), (0,0.5), (0.5,0), (0.5,0.5)\}$, and it is assumed that the estimation of the subpixel motion is incorrect as $\{(0,0), (0,0.3), (0.4,0.1), (0.8,0.6)\}$. Figure 13 is a partially magnified image of the result of a conventional SR algorithm that does not consider the registration error (i.e., a constant regularization parameter is used). The partially magnified image of the result by employing channel adaptive regularization in which the registration error is considered via $\lambda_k(\mathbf{x})$ is shown in Figure 13(b). The results in Figure 13 visually show that the method considering the registration errors yields better performance than the conventional approach.

A simultaneous registration and reconstruction approach [20], [22], [59] is also expected to reduce the effect of registration error in the SR estimates, since registration and reconstruction process are closely interdependent.

Blind SR Image Reconstruction

In most SR reconstruction algorithms, the blurring process is assumed to be known. In many practical situations, however, the blurring process is generally unknown or is known only to within a set of parameters. Therefore, it is necessary to incorporate the blur identification into the reconstruction procedure.

Wirawan et al. [47] proposed a blind multichannel SR algorithm by using multiple finite impulse response (FIR) filters. Since each observed image is a linear combination of the polyphase components of the HR image, the SR problem can be represented as the blind 2-D multi-input, multi-output (MIMO) system driven by polyphase components of a bandlimited signal. Their algorithm consists of two stages: blind 2-D MIMO deconvolution using FIR filters and separation of mixed polyphase components. A mutually referenced equalizer (MRE) algorithm is extended to solve the blind multichannel deconvolution problem. Since blind MIMO deconvolution based on second-order statistics contains some inherent indeterminations, the polyphase components need to be separated after deconvolution. They proposed a source separation algorithm which minimizes out-of-band spectral energy resulting from instantaneous mixture of polyphase components.

Nguyen et al. [48] proposed a technique for parametric blur identification and regularization based on the generalized cross-validation (GCV) and Gauss quadrature theory. They solve a multivariate nonlinear minimization problem for these unknown parameters. To efficiently and accurately estimate the numerator and denominator of the GCV objective function, Gauss-type quadrature techniques for bounding quadratic forms are used.

### Computationally Efficient SR Algorithm

The inverse procedure in SR reconstruction obviously requires a very large computational load. To apply the SR algorithm to practical situations, it is important to develop an efficient algorithm that reduces the computational cost. As mentioned earlier, the interpolation-based approach and adaptive filtering approach can be appropriate to real-time implementation. Another effort concerning this issue is found in [49]-[51].

Nguyen et al. [49] proposed a circulant block preconditioners to accelerate the conjugate gradient methods for solving the Tikhonov-regularized SR problem. This preconditioning technique transforms the original system into another system in which rapid convergence is possible without any change in the solution. Generally, since the convergence rate of CG depends on the distribution of the eigenvalues of the system matrix $\mathbf{W_k}$, for the purpose of fast convergence, a preconditioned system with eigenvalues clustering around one is derived. These preconditioners can be easily realized, and the operation with these preconditioners can be done efficiently by using a 2-D fast Fourier transform.

Elad and Hel-Or [50] proposed an SR algorithm that separates fusion and deblurring. To reduce computational load, they assume that the blur is space invariant and the same for all the observed images, the geometric warps between the measured images are modeled as only pure translations, and the additive noise is white. Although these assumptions are limited, the proposed fusion method is achieved through a very simple noniterative algorithm, while preserving its optimality in the ML sense.

Concluding Remarks

We tried to address the concept of SR technology in this article by providing an overview of existing SR algorithms and advanced issues currently under investigation. Other issues in the SR techniques to improve their performance are currently focused on the color SR algorithm and the application to compression systems. It is necessary to extend the current SR algorithm

(a)   (b)
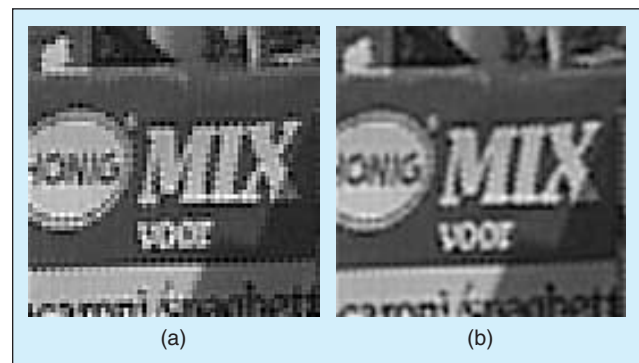
▲ 13. The effect of registration error in HR estimate; result by (a) the conventional algorithm and (b) the channel-adaptive regularization.

Robustness and flexibility in modeling noise characteristics and a priori knowledge about the solution are the major advantages of the stochastic SR approach.

to a real-world color imaging system. A color SR application is considered in [8], [31], and [52]-[55], but a more careful reconstruction method which reflects the characteristic of color is needed. The important problem in color SR is to analyze the characteristic of a color filter array and color interpolation procedure and take into account intercorrelation between color components in the reconstruction procedure. The application of the SR algorithm to the compression system is also needed [4], [56]-[61], since images are routinely compressed prior to transmission and storage. In this case, the SR algorithm must account for the structure of the compression system. For example, it is important to analyze and model the compression error caused by quantization, since a simple Gaussian noise model is not acceptable, especially when a significant amount of compression is employed.

SR image reconstruction is one of the most spotlighted research areas, because it can overcome the inherent resolution limitation of the imaging system and improve the performance of most digital image processing applications. We hope this article creates interest in this area as well as inspiration to develop the relevant techniques.

Acknowledgment

Sung Cheol Park received the B.S. and M.S. degrees in electronics engineering from Yonsei University, Korea, in 1998 and 2000, respectively. He is currently pursuing the Ph.D. degree. His current research interests include image and video filtering, restoration, and reconstruction.

Min Kyu Park received the B.S. and M.S. degrees in electronics engineering from Yonsei University, Korea, in 1999 and 2001, respectively. He is currently pursuing the Ph.D. degree. His current research interests include motion estimation, super resolution, and deinterlacing.

Moon Gi Kang received the B.S. and M.S. degrees in electronics engineering from Seoul National University, Korea, in 1986 and 1988, respectively, and the Ph.D. degree in electrical engineering from Northwestern University in 1994. He was an assistant professor at the University of Minnesota, Duluth, from 1994 to 1997, and since 1997 he has been in the Department of Electronic Engineering, Yonsei University, Seoul, Korea, where he is currently an associate professor. His current research interests include image and video filtering, restoration, enhancement, and reconstruction. He has published more than 80 technical articles in these areas. He is a member of IEEE and SPIE. He served on the editorial board of *IEEE Signal Processing Magazine*, editor of SPIE Milestone Series (CCD and CMOS imagers), guest editor of the *IEEE Signal Processing Magazine* special section on super-resolution image reconstruction (May 2003), and reviewer for *IEEE Transactions on Image Processing*. He has served in the technical program and steering committees of several international conferences. He has also served domestically as the associate editor for *Journal of Broadcast Engineering* and *Journal of IEEK* (the Institute of Electronics Engineers of Korea).

References

[1] T. Komatsu, K. Aizawa, T. Igarashi, and T. Saito, "Signal-processing based method for acquiring very high resolution image with multiple cameras and its theoretical analysis," *Proc. Inst. Elec. Eng.*, vol. 140, no. 1, pt. I, pp. 19-25, Feb. 1993.

[2] S. Borman and R.L. Stevenson, "Spatial resolution enhancement of low-resolution image sequences. A comprehensive review with directions for future research," Lab. Image and Signal Analysis, University of Notre Dame, Tech. Rep., 1998.

[3] S. Borman and R.L. Stevenson, "Super-resolution from image sequences—A review," in *Proc. 1998 Midwest Symp. Circuits and Systems,* 1999, pp. 374-378.

[4] S. Chaudhuri, Ed., *Super-Resolution Imaging*. Norwell, MA: Kluwer, 2001.

[5] H. Ur and D. Gross, "Improved resolution from sub-pixel shifted pictures," *CVGIP: Graphical Models and Image Processing*, vol. 54, pp. 181-186, Mar. 1992.

[6] T. Komatsu, T. Igarashi, K. Aizawa, and T. Saito, "Very high resolution imaging scheme with multiple different-aperture cameras," *Sinal Processing: Image Commun.,* vol. 5, pp. 511-526, Dec. 1993.

[7] M.S. Alam, J.G. Bognar, R.C. Hardie, and B.J. Yasuda, "Infrared image registration and high-resolution reconstruction using multiple translationally shifted aliased video frames," *IEEE Trans. Instrum. Meas.*, vol. 49, pp. 915-923, Oct. 2000.

[8] N.R. Shah and A. Zakhor, "Resolution enhancement of color video sequences," *IEEE Trans. Image Processing,* vol. 8, pp. 879-885, June 1999.

[9] N. Nguyen and P. Milanfar "An efficient wavelet-based algorithm for image superresolution," in *Proc. Int. Conf. Image Processing*, vol. 2, 2000, pp. 351-354.

[10] R.Y. Tsai and T.S. Huang, "Multipleframe image restoration and registration," in *Advances in Computer Vision and Image Processing*. Greenwich, CT: JAI Press Inc., 1984, pp. 317-339.

[11] S.P. Kim, N.K. Bose, and H.M. Valenzuela, "Recursive reconstruction of high resolution image from noisy undersampled multiframes," *IEEE Trans. Acoust., Speech, Signal Processing*, vol. 38, pp. 1013-1027, June 1990.

[12] S.P. Kim and W.Y. Su, "Recursive high-resolution reconstruction of blurred multiframe images," *IEEE Trans. Image Processing,* vol. 2, pp. 534-539, Oct. 1993.

[13] N.K. Bose, H.C. Kim, and H.M. Valenzuela, "Recursive implementation of total least squares algorithm for image reconstruction from noisy, undersampled multiframes," in *Proc. IEEE Conf. Acoustics, Speech and Signal Processing,* Minneapolis, MN, Apr. 1993, vol. 5, pp. 269-272.

[14] S.H. Rhee and M.G. Kang, "Discrete cosine transform based regularized high-resolution image reconstruction algorithm," *Opt. Eng.,* vol. 38, no. 8, pp. 1348-1356, Aug. 1999.

[15] M.C. Hong, M.G. Kang, and A.K. Katsaggelos, "A regularized multi-channel restoration approach for globally optimal high resolution video sequence," in *SPIE VCIP,* vol. 3024, San Jose, CA, Feb. 1997, pp. 1306-1317.

[16] M.C. Hong, M.G. Kang, and A.K. Katsaggelos, "An iterative weighted regularized algorithm for improving the resolution of video sequences," in *Proc. Int. Conf. Image Processing,* vol. 2, 1997, pp. 474-477.

[17] M.G. Kang, "Generalized multichannel image deconvolution approach and its applications," *Opt. Eng.,* vol. 37, no. 11, pp. 2953-2964, Nov. 1998.

[18] R.C. Hardie, K.J. Barnard, J.G. Bognar, E.E. Armstrong, and E.A. Watson, "High-resolution image reconstruction from a sequence of rotated and translated frames and its application to an infrared imaging system," *Opt. Eng.,* vol. 37, no. 1, pp. 247-260, Jan. 1998.

[19] N.K. Bose, S. Lertrattanapanich, and J. Koo, "Advances in superresolution using L-curve," in *Proc. Int. Symp. Circuits and Systems*, vol. 2, 2001, pp. 433-436.

[20] B.C. Tom and A.K. Katsaggelos, "Reconstruction of a high-resolution image by simultaneous registration, restoration, and interpolation of low-resolution images," *Proc. 1995 IEEE Int. Conf. Image Processing,* vol. 2, Washington, DC, Oct. 1995, pp. 539-542.

[21] R.R. Schulz and R.L. Stevenson, "Extraction of high-resolution frames from video sequences," *IEEE Trans. Image Processing*, vol. 5, pp. 996-1011, June 1996.

[22] R.C. Hardie, K.J. Barnard, and E.E. Armstrong, "Joint MAP registration and high-resolution image estimation using a sequence of undersampled images," *IEEE Trans. Image Processing.*, vol. 6, pp. 1621-1633, Dec. 1997.

[23] P. Cheeseman, B. Kanefsky, R. Kraft, J. Stutz, and R. Hanson, "Super-resolved surface reconstruction from multiple images," NASA Ames Research Center, Moffett Field, CA, Tech. Rep. FIA-94-12, Dec. 1994.

[24] H. Stark and P. Oskoui, "High resolution image recovery from image-plane arrays, using convex projections," *J. Opt. Soc. Am. A,* vol. 6, pp. 1715-1726, 1989.

[25] A.M. Tekalp, M.K. Ozkan, and M.I. Sezan, "High-resolution image reconstruction from lower-resolution image sequences and space varying image restoration," in *Proc. IEEE Int. Conf. Acoustics, Speech and Signal Processing (ICASSP),* San Francisco, CA., vol. 3, Mar. 1992, pp. 169-172.

[26] A.J. Patti, M.I. Sezan, and A.M. Tekalp, "Superresolution video reconstruction with arbitrary sampling lattices and nonzero aperture time," *IEEE Trans. Image Processing,* vol. 6, no. 8, pp. 1064-1076, Aug. 1997.

[27] P.E. Eren, M.I. Sezan, and A.M. Tekalp, "Robust, object-based high-resolution image reconstruction from low-resolution video," *IEEE Trans. Image Processing,* vol. 6, no. 10, pp. 1446-1451, Oct. 1997.

[28] A.J. Patti and Y. Altunbasak, "Artifact reduction for set theoretic super resolution image reconstruction with edge adaptive constraints and higher-order interpolants," *IEEE Trans. Image Processing,* vol. 10, no. 1, pp. 179-186, Jan. 2001.

[29] B.C. Tom and A.K. Katsaggelos "An iterative algorithm for improving the resolution of video sequences," in *Proc. 1996 SPIE Conf. Visual Communications and Image Processing*, Orlando, FL, Mar. 1996, pp. 1430-1438.

[30] M. Elad and A. Feuer, "Restoration of a single superresolution image from several blurred, noisy, and undersampled measured images," *IEEE Trans. Image Processing,* vol. 6 , no. 12, pp. 1646-1658, Dec. 1997.

[31] M. Irani and S. Peleg, "Improving resolution by image registration," *CVGIP: Graphical Models and Image Proc.,* vol. 53, pp. 231-239, May 1991.

[32] S. Mann and R.W. Picard, "Virtual bellows: Constructing high quality stills from video," in *Proc. IEEE Int. Conf. Image Processing,* Austin, TX, Nov. 1994, pp. 13-16.

[33] M. Irani and S. Peleg, "Motion analysis for image enhancement resolution, occlusion, and transparency," *J. Visual Commun. Image Represent.,* vol. 4, pp. 324-335, Dec. 1993.

[34] M. Elad and A. Feuer, "Superresolution restoration of an image sequence: adaptive filtering approach," *IEEE Trans. Image Processing,* vol. 8, pp. 387-395, Mar. 1999.

[35] M. Elad and A. Feuer, "Super-resolution reconstruction of image sequences," *IEEE Trans. Pattern Anal. Machine Intelli.*, vol. 21, no. 9, pp. 817-834, Sept. 1999.

[36] M.C. Chiang and T.E. Boult, "Efficient super-resolution via image warping," *Image Vision Computing*, vol. 18, pp. 761-771, Dec. 2000.

[37] D. Rajan and S. Chaudhuri, "Generation of super-resolution images form blurred observations using an MRF model," *J. Math. Imaging Vision,* vol. 16, pp. 5-15, 2002.

[38] D. Rajan and S. Chaudhuri, "Simultaneous estimation of super-resolved intensity and depth maps from low resolution defocused observations of a scene," in *Proc. IEEE int. Conf. Computer Vision*, Vancouver, Canada, July 2001, pp. 113-118.

[39] D. Rajan and S. Chaudhuri, "Generalized interpolation and its applications in super-resolution imaging," *Image and Vision Computing,* vol. 19, pp. 957-969, Nov. 2001.

[40] M.V. Joshi and S. Chaudhuri, "Super-resolution imaging: Use of zoom as a cue," in *Proc. Indian Conf. Vision, Graphics and Image Processing*, Ahmedabad, India, Dec. 2002, pp. 439-444.

[41] N.K. Bose, H.C. Kim, and B. Zhou, "Performance analysis of the TLS algorithm for image reconstruction from a sequence of undersampled noisy and blurred frames," in *Proc. ICIP-94, IEEE Int. Conf. Image Processing,* vol. 3, 1994, pp. 571-575.

[42] M. Ng, J. Koo, and N. Bose, "Constrained total least squares computations for high resolution image reconstruction with multisensors," *Int. J. Imaging Syst. Technol.,* vol. 12, pp. 35-42, 2002.

[43] M.K. Ng and N.K. Bose, "Analysis of displacement errors in high-resolution image reconstruction with multisensors," *IEEE Trans. Circuits Syst. I,* vol. 49, pp. 806-813, June 2002.

[44] M. Park, E. Lee, J. Park, M.G. Kang, and J. Kim, "DCT-based high-resolution image reconstruction considering the inaccurate sub-pixel motion information," *SPIE Optical Engineering,* vol. 41, no. 2, pp. 370-380, Feb. 2002.

[45] W. Lim, M. Park, and M.G. Kang, "Spatially adaptive regularized iterative high resolution image reconstruction algorithm," in *Proc. VCIP2001, Photonicswest,* San Jose, CA, Jan. 2001, pp. 20-26.

[46] E. Lee and M.G. Kang, "Regularized adaptive high-resolution image reconstruction considering inaccurate subpixel registration," *IEEE Trans. Image Processing*, to be published.

[47] Wirawan, P. Duhamel, and H. Maitre, "Multi-channel high resolution blind image restoration," in *Proc. IEEE ICASSP,* AZ, Nov. 1989, pp. 3229-3232.

[48] N. Nguyen, P. Milanfar, and G. Golub, "Efficient generalized cross-validation with applications to parametric image restoration and resolution enhancement," *IEEE Trans. Image Processing,* vol. 10, pp. 1299-1308, Sept. 2001.

[49] N. Nguyen, P. Milanfar, and G. Golub, "A computationally efficient superresolution image reconstruction algorithm," *IEEE Trans. Image Processing,* vol. 10, pp. 573-583, Apr. 2001.

[50] M. Elad and Y. Hel-Or, "A fast super-resolution reconstruction algorithm for pure translational motion and common space-invariant blur," *IEEE Trans. Image Processing,* vol. 10, no. 8, pp. 1187-1193, Aug. 2001.

[51] M. Ng, R. Chan, T. Chan, and A.Yip, "Cosine transform preconditioners for high resolution image reconstruction," *Linear Algebra Appls.*, vol. 316, pp. 89-104, 2000.

[52] D.S. Messing and M.I. Sezan, "Improved multi-image resolution enhancement for colour images captured by single-CCD cameras," in *Proc. Int. Conf. Image Processing*, vol. 3, 2000, pp. 484-487.

[53] M.K. Ng, "An efficient parallel algorithm for high resolution color image reconstruction," in *Proc. 7th Int. Conf. Parallel and Distributed Systems: Workshops,* 2000, pp. 547-552.

[54] B.C. Tom and A.K. Katsaggelos, "Resolution enhancement of monochrome and color video using motion compensation," *IEEE Trans. Image Processing,* vol. 10, no. 2, pp. 278-287, Feb. 2001.

[55] M. Ng and W. Kwan, "High-resolution color image reconstruction with Neumann boundary conditions," *Ann. Oper. Res.,* vol. 103, pp. 99-113, 2001.

[56] D. Chen and R.R. Schultz, "Extraction of high-resolution video stills from MPEG image sequences," in *Proc. 1998 IEEE Int. Conf. Image Processing,* vol. 2, 1998, pp. 465-469.

[57] Y. Altunbasak and A.J. Patti, "A maximum a posteriori estimator for high resolution video reconstruction from MPEG video," in *Proc. 2000 IEEE Int. Conf. Image Processing,* vol. 2, 2000, pp. 649-652.

[58] B. Martins and S. Forchhammer, "A unified approach to restoration, deinterlacing and resolution enhancement in decoding MPEG-2 video," *IEEE Trans. Circuits Syst. Video Technol.,* vol. 12, no. 9, pp. 803-811, Sept. 2002.

[59] C.A. Segall, R. Molina, A.K. Katsaggelos, and J. Mateos, "Reconstruction of high-resolution image frames from a sequence of low-resolution and compressed observations," in *Proc. 2002 IEEE Int. Conf. Acoustics, Speech, and Signal Processing,* vol. 2, 2002, pp. 1701-1704.

[60] S.C. Park, M.G. Kang, C.A. Segall, and A.K. Katsaggelos, "Spatially adaptive high-resolution image reconstruction of low resolution DCT-based compressed images," in *Proc. 2002 IEEE Int. Conf. Image Processing,* vol. 2, 2002, pp. 861-864.

[61] B.K. Gunturk, Y. Altunbasak, and R.M. Mersereau, "Multiframe resolution-enhancement methods for compressed video," *IEEE Signal Processing Lett.,* vol. 9, pp. 170-174, June 2002.

[62] H.C. Andrews and B.R. Hunt, *Digital Image Restoration*. Englewood Cliffs, NJ: Prentice-Hall, 1977.

[63] A.K. Katsaggelos, Ed. *Digital Image Restoration.* Heidelberg, Germany: Springer-Verlag. Springer. vol. 23, 1991.

[64] I.J. Schoenberg, "Cardinal interpolation and spline functions," *J. Approx. Theory.*, vol. 2, pp. 167-206, 1969.

[65] R.E. Crochiere and L.R. Rabiner, "Interpolation and decimation of digital signals—A turorial review," *Proc. IEEE*, vol. 69, no. 3, pp. 300-331, Mar. 1981.

[66] M. Unser, A. Aldroubi, and M. Eden, "Enlargement or reduction of digital images with minimum loss of information," *IEEE Trans. Image Processing*, vol. 4, no. 3, pp. 247-258, Mar. 1995.

[67] V.N. Dvorchenko, "Bounds on (deterministic)correlation functions with applications to registration." *IEEE Trans. Pattern Anal. Machine Intell.*, vol. 5, no. 2. pp. 206-213, 1983.

[68] Q. Tian and M.N. Huhns, "Algorithm for subpixel registration," *Computer Vision, Graphics, Image Proc.,* vol. 35, pp. 220-233, 1986.

[69] C.A. Bernstein, L.N. Kanal, D. Lavin, and E.C. Olson, "A geometric approach to subpixel registration accuracy," *Computer Vsion, Graphics, and Image Proc.,* vol. 40, pp. 334-360, 1987.

[70] L.G. Brown, "A survey of image registration techniques," *ACM Comput. Surveys,* vol. 24, no. 4, pp. 325-376, Dec. 1992.

[71] J. J. Clark, M R. Palmer, and P.D. Laurence, "A transformation method for the reconstruction of functions from nonuniformly spaced samples," *IEEE Trans. Acoust., Speech, Signal Processing,* vol. ASSP-33, pp. 1151-1165, 1985.

[72] S.P. Kim and N.K. Bose, "Reconstruction of 2-D bandlimited discrete signals from nonuniform samples," *Proc. Inst. Elec. Eng.,* vol. 137, pt. F, pp. 197-204, June 1990.

[73] A. Papoulis, "Generalized sampling theorem," *IEEE Trans. Circuits Syst.* vol. 24, pp. 652-654, Nov. 1977.

[74] J.L. Brown, "Multi-channel sampling of low pass signals," *IEEE Trans. Circuits Syst.,* vol. CAS-28, pp. 101-106, Feb. 1981.

[75] L. Landweber, "An iteration formula for Fredholm integral equations of the first kind," *Amer. J. Math.* vol. 73, pp. 615-624, 1951.

[76] A.M. Tekalp, *Digital Video Processing*. Englewood Cliffs, NJ: Prentice Hall, 1995.

[77] P.C. Hansen, and D. Prost O'Leary, "The use of the L-curve in the regularization of discrete ill-posed problems," *SIAM J. Sci. Comput.,* vol. 14, no. 6, pp. 1487-1503, Nov. 1993.

[78] H.J. Trussell and M.T. Civanlar, "Feasible solution in signal restoration," *IEEE Trans. Acoust., Speech, Signal Processing,* vol. ASSP-32, pp. 201-212, Mar. 1984.

[79] M.G. Kang and A.K. Katsaggelos, "General choice of the regularization functional in regularized image restoration," *IEEE Trans. Image Processing*, vol. 4, pp. 594-602, May 1995.